ChemComm

COMMUNICATION

View Article Online
View Journal | View Issue

Cite this: *Chem. Commun.*, 2023, 59, 6560

Received 20th February 2023,
Accepted 2nd May 2023

DOI: 10.1039/d3cc00784g

rsc.li/chemcomm

Bilateral π-extension of an open-[60]fullerene in a helical manner†

Yoshifumi Hashikawa, Shumpei Sadai and Yasujiro Murata *

The conventional π-elongation of open-[60]fullerenes could only give unilaterally π-extended derivatives. Herein, we report the further π-elongation at another site to achieve bilateral π-elongation *via* a consecutive nucleophilic addition of 4,5-dimethyl-*o*-phenylenediamine. The thus-formed π-extended open-[60]fullerene bears two-fold diaza[*n*]helicene (*n* = 5 and 6) motifs in its skeleton. The crystallographic analysis revealed the characteristic helicene–fullerene interactions with close contacts of 3.09 and 3.14 Å.

Open-[60]fullerenes[1] contain a geodesic polyarene with a formula of $C_{50}H_{10}$, which was firstly synthesized as the shortest end-cap (5,5) carbon nanotube (CNT) by Scott and co-workers in 2012.[2] The (5,5) end-cap is a possible template molecule for CNT growth. The chemical vapor deposition in the presence of a mixed carbon source of CH_4/C_2H_4 indeed produced single-walled CNTs with an average diameter of 0.82 nm.[3] The similar preprogrammed bottom-up synthesis of CNTs has been demonstrated using unimolecular seeds such as cycloparaphenylene,[4] truxene derivative,[5] and open-[60]fullerene,[6] in which ethanol is usually employed as a carbon source. These methods enable the production of CNTs with atomically-controlled diameters. However, the bay regions in the (5,5) end-cap resist Diels–Alder cycloadditions, thus being far less reactive toward nitroethylene and benzyne.[7] Therefore, organic synthesis of molecular CNTs with an atomically precise π-conjugation length still remains a formidable challenge.

The consecutive chemical scission of [60]fullerene gives an open-form with a large orifice.[1] This type of open-[60]fullerene could be regarded as a functional π-extended (5,5) end-cap (Fig. 1). Apart from the pristine (5,5) end-cap with a poor reactivity, open-[60]fullerenes are expected to be promising seeds for the growth of molecular CNTs.[8] The unilateral π-extension of open-[60]fullerenes has been developed by Iwamatsu[9] and us,[10] independently, in which a fused quinoxaline was introduced to the geodesic π-conjugation (Fig. 1). The related conjugation motifs of such acceptor–acceptor (quinoxaline–open-[60]fullerene) hybrids were also prepared by Gan and co-workers.[11] Recently, we synthesized π-extended open-[60]fullerenes with a fused imidazole (Fig. 1),[10b] showing a notable increase of the absorption coefficients in the visible region owing to donor–acceptor interactions.[12] As exemplified above, open-[60]fullerenes allow us to precisely elongate their π-skeleton in a step-by-step manner while the unilateral π-elongation provides molecular platforms not ideal for the construction of tubular nanostructures. Thereby, multilateral and/or uniform π-elongation from the rim is highly demanded to chemically synthesize molecular CNTs. Herein, we report a bilateral π-elongation of an open-[60]fullerene, giving access to a π-extended (5,5) end-cap with two-fold embedded hetero[*n*]helicene motifs.

Recently, we have reported a unilateral π-elongation of an open-[60]fullerene giving tricarbonyl derivative **1** (Scheme 1).[10a] We had initially expected the further π-elongation from C(1)═O(1) and C(4)═O(4) groups as footholds *via* two-fold dehydrative condensation with a suitable aromatic diamine. Thus, the reaction of **1** with 4,5-dimethyl-*o*-phenylenediamine

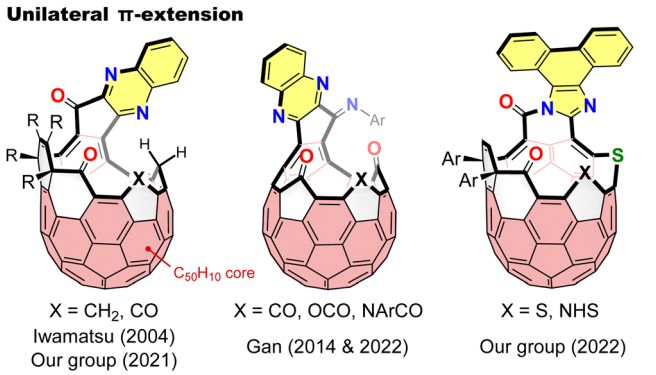

Fig. 1 Unilateral π-extension of open-[60]fullerenes.

Institute for Chemical Research, Kyoto University, Uji, Kyoto 611-0011, Japan. E-mail: yasujiro@scl.kyoto-u.ac.jp

† Electronic supplementary information (ESI) available: Detailed synthetic procedures, spectra, and optimized geometries. CCDC 2236614. For ESI and crystallographic data in CIF or other electronic format see DOI: https://doi.org/10.1039/d3cc00784g

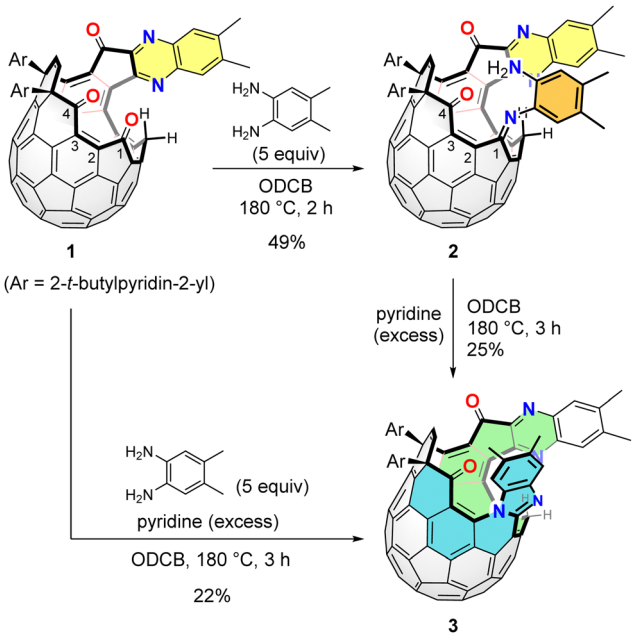

Scheme 1 Synthesis of **3**.

was conducted in *o*-dichlorobenzene (ODCB) at 180 °C for 2 h. As a result, **2** was obtained in 49% isolated yield by a single dehydrative condensation, while the further reaction did not proceed at all (Scheme 1). The high selectivity at the C(1)═O(1) group is simply due to its higher accessibility (Fig. 2a). With the key precursor (**2**) in hand, we then tried the reaction in the presence of pyridine. The mass spectrometric analysis of the product (**3**) showed a molecular ion peak at *m*/*z* 1336.3477, which differs from the initially expected compound ($[\mathbf{2}–H_2O]^{\bullet-}$) but was finally assignable to $[\mathbf{2}–2H]^{\bullet-}$. The absence of the amino group was confirmed by ^{1}H NMR while ^{13}C NMR spectrum of **3** (201 MHz, acetone-d_6/CS_2 (1 : 5)) clearly indicated the presence of two carbonyl groups at δ 192.00 and 187.42 ppm. These results imply that the reaction occurred at the rim of the orifice undoubtedly with the amino group. The structure of **3** was unambiguously determined by X-ray crystallographic analysis (Fig. 3) and found to have an imidazole ring generated through a nitrogen-insertion between the C(1)–C(2) bond. Upon seeing the LUMO+1, the large orbital coefficient was found at the α,β-unsaturated carbonyl group where the C(2) atom (q_{NPA} +0.016) is more positively charged rather than C(3) (q_{NPA} −0.079) according to the natural population analysis (NPA) (Fig. 2b). Note that the LUMO

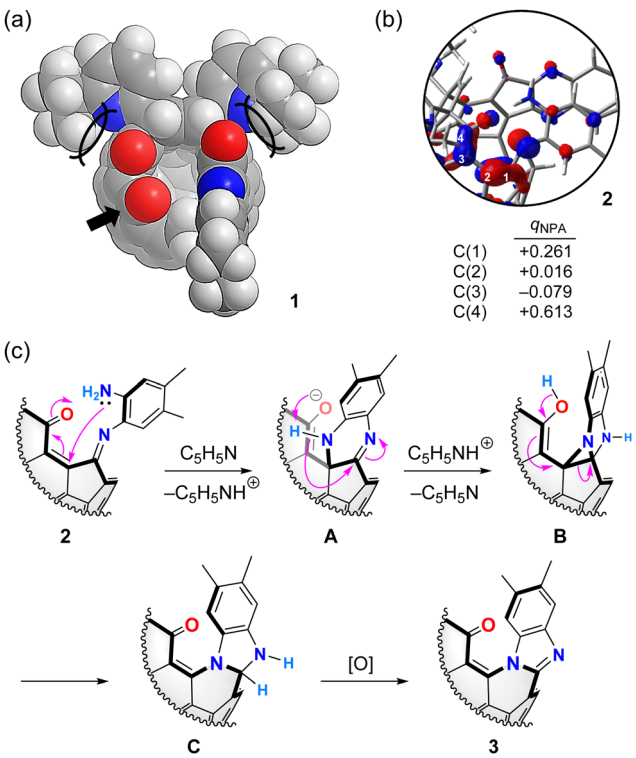

Fig. 2 (a) Optimized structure of **1**, (b) the LUMO+1 of **2** and natural charges q_{NPA} of selected carbon atoms, and (c) plausible mechanism. The calculations were performed at the B3LYP-D3/6-31G(d) level of theory.

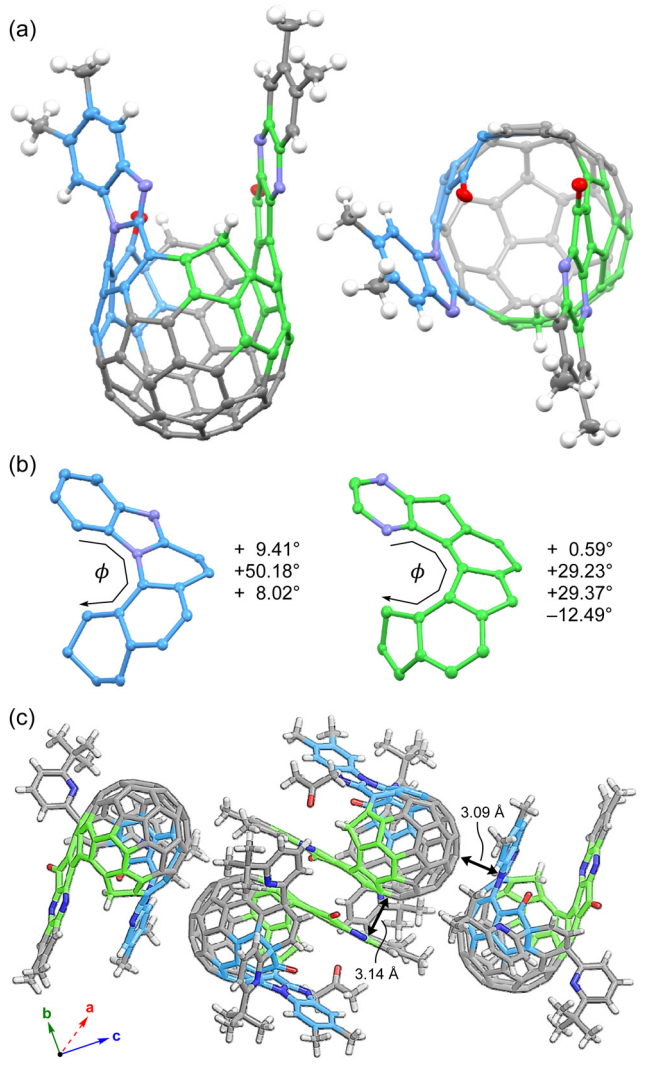

Fig. 3 Single crystal X-ray structures of **3**: (a) side and top views (the aryl groups are omitted for clarity), (b) embedded helical motifs with torsion angles φ along helical inner rims, and (c) packing view with contact distances. The solvent and encapsulated molecules are not shown for all views.

has large coefficients on the entire [60]fullerene skeleton. As is the case with the addition of the diamine to **1**, the amino group in **2** is not likely to attack the C(4)═O(4) group due to the steric demand while it undergoes a nucleophilic addition to the C(2) atom, thus giving intermediate **A** which is transformed into **B** *via* aziridination (Fig. 2c). The subsequent ring-opening reaction allows for the nitrogen atom to be inserted into the rim of the orifice. The thus-formed dihydroimidazole derivative (**C**) is then oxidized to afford imidazole-fused **3**.

The single crystals of racemic **3** were obtained from a CS_2/acetone solution. The solid-state structure for one of the two enantiomers is shown in Fig. 3. It is worth mentioning that the π-elongation was achieved on the geodesic [60]fullerene skeleton in a bilateral manner (Fig. 3a) where the two π-systems are embedded as diaza[*n*]helicenes (*n* = 5 and 6) with a single *P*-helicity (Fig. 3b), while another enantiomer consists of a single *M*-helicity. The torsion angles φ along the helical inner rims indicate the considerably larger distortion of the two helical motifs, when compared with non-substituted carbo[5] and [6]helicenes (16.4, 31.5, and 18.4° and 11.1, 30.1, 31.2, and 15.1°),[13] reflecting the positive curvature of the [60]fullerene skeleton. Within the crystal, the molecules of **3** are arranged in close proximity with contact distances of 3.09 and 3.14 Å between the helically and spherically π-conjugated motifs (Fig. 3c).

We also examined the chemical transformation of **2** at the amino group (Scheme 2). The reaction of **2** with trifluoroacetic acid smoothly gave the corresponding amide **4** in 88% yield under catalyst-free conditions. Such condensation is known to occur only if aniline is substituted with an electron-deficient group, which prevents it from generating a salt with the acid.[14] In our case, the strong electron-accepting character of the [60]fullerene moiety is considered to make catalysts unnecessary. As another electrophile, we used *p*-tolyl isocyanate, which furnished the corresponding urea derivative **5** in 35% isolated yield together with **3** (27%).

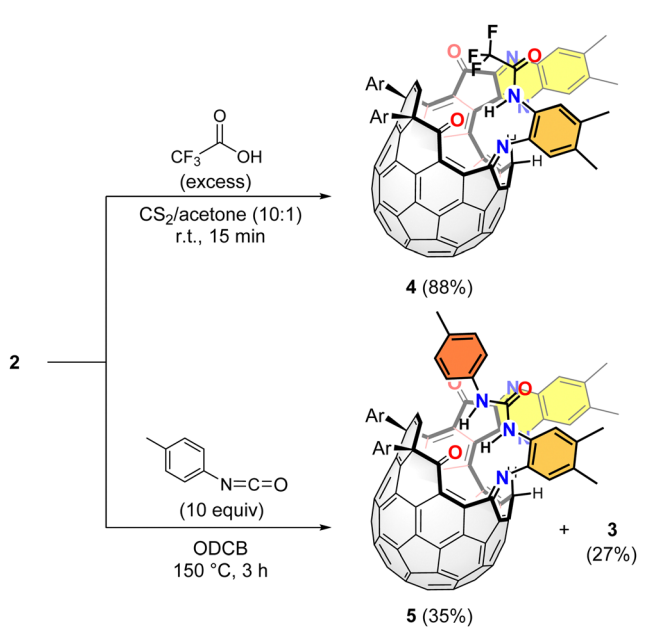

Scheme 2 Synthesis of **4** and **5**.

To get insights into the electronic properties of **1**–**5**, we measured absorption spectra in benzene (Fig. 4). Compound **6**,[15] which bears two carbonyl groups, was also measured as a reference molecule for evaluating the effect of the π-elongation in **1** and **3**. As shown in Fig. 4a, the first π-elongation (**6** → **1**) drastically modulates the absorption properties with increased coefficients over the measured range. The embedded diaza[6]helicene moiety in **1** is well-conjugated with the [60]fullerene skeleton as found in the HOMO–1 and LUMO (B3LYP/6-31G(d)) (Fig. 4c). The second π-elongation (**1** → **3**) contributes to a slight increase in absorption at the visible region (Fig. 4a). According to theoretical calculations (Fig. 4c), the HOMO of **3** (−5.48 eV) is dominantly distributed on the aza[5]helicene moiety, which is less conjugated with the [60]fullerene core, while it overrides the level of the original HOMO (−5.69 eV) of **1** by the second π-elongation. The longest wavelength absorption of **3** originates from a charge transfer transition as opposed to **1** showing

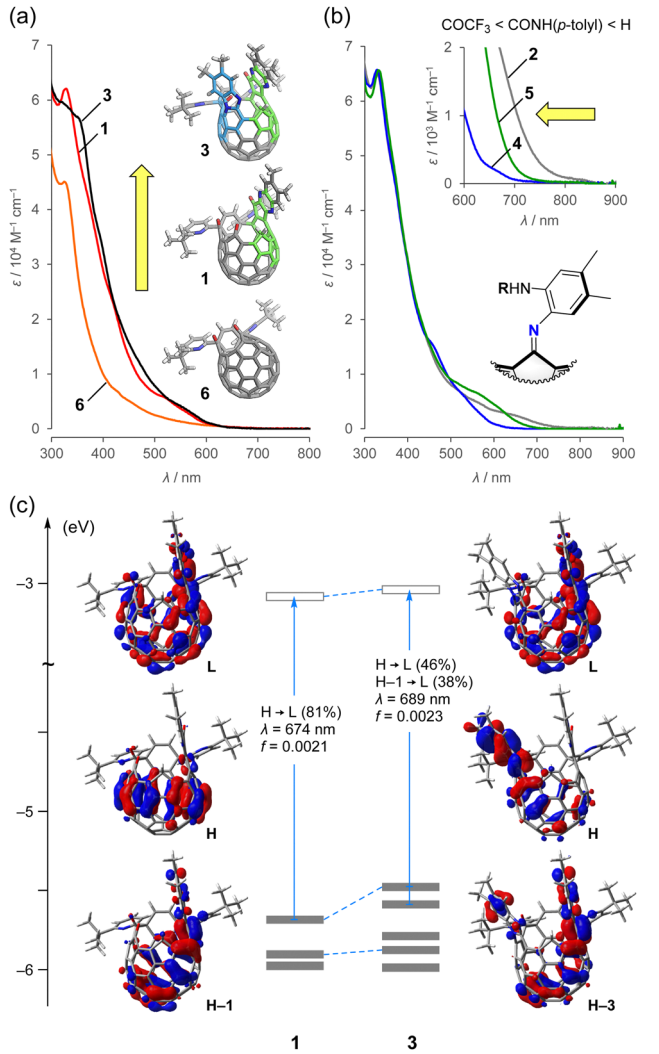

Fig. 4 UV-vis-NIR absorption spectra of (a) **1**, **3**, and **6** and (b) **2**, **4**, and **5** (50 μM in benzene). (c) Kohn–Sham HOMO and LUMO levels of **1** and **3** with optical transitions (TD CAM-B3LYP/6-31G(d)//B3LYP/6-31G(d)). The transition energies were calibrated with a factor of 0.72.[16]

a π–π* character. Note that the HOMO–3 (−5.88 eV) and LUMO (−3.04 eV) of **3** bear a close resemblance with the HOMO–1 (−5.91 eV) and LUMO (−3.09 eV) of **1**, respectively, without considerable perturbation to their energy levels by the second π-elongation.

The aniline-substituted derivative (**2**) exhibited a near-infrared (NIR) absorption, which tails to 870 nm (Fig. 4b). The absorption edges were hypochromically shifted by varying the substituents: amide (**4**, 750 nm) < urea (**5**, 800 nm) < amine (**2**, 870 nm). The theoretical calculations suggested that the HOMO level is lowered in the order of **2** (−4.96 eV) > **5** (−5.06 eV) > **4** (−5.65 eV), while the LUMO levels are comparable (**2**, −2.97 eV; **5**, −3.12 eV; **4**, −3.08 eV) (B3LYP/6-31G(d)). Thus, the observed hypsochromic shift is ascribed to the magnitude of the donor character on the aniline moiety in **2**, **4**, and **5**.

In summary, we achieved the second π-elongation of a unilaterally π-extended open-[60]fullerene (**1**) by the reaction with 4,5-dimethyl-*o*-phenylenediamine in the presence of pyridine. The structure of the product (**3**) was unambiguously determined by X-ray diffraction analysis, which revealed the bilateral π-elongation from the [60]fullerene core in a helical manner. The two embedded diaza[*n*]helicene (*n* = 5 and 6) moieties are severely distorted due to the positive curvature of the [60]fullerene skeleton. The close contacts between the helical and spherical π-motifs were found at distances of 3.09 and 3.14 Å. In this reaction, **2** is a key intermediate for the formation of **3** and its electronic structure was found to be modifiable by the reaction with electrophiles, thus observing the obvious hypochromic shift in the absorption spectra. Since **3** could be regarded as a π-extended (5,5) end-cap, this approach would open a way to create structurally well-defined molecular CNTs through stepwise chemical reactions.

Financial support was partially provided by the JSPS KAKENHI Grant Number JP17H06119 and JP22H04538, ISHIZUE 2022 of Kyoto University, and The Mazda Foundation. The NMR measurements were partly supported by the Joint Usage/Research Center (JURC) at the ICR, Kyoto University.

Conflicts of interest

There are no conflicts to declare.

Notes and references

1 (*a*) M. Murata, Y. Murata and K. Komatsu, *Chem. Commun.*, 2008, 6083–6094; (*b*) G. C. Vougioukalakis, M. M. Roubelakis and M. Orfanopoulos, *Chem. Soc. Rev.*, 2010, **39**, 817–844; (*c*) L. Shi and L. Gan, *J. Phys. Org. Chem.*, 2013, **26**, 766–772.
2 L. T. Scott, E. A. Jackson, Q. Zhang, B. D. Steinberg, M. Bancu and B. Li, *J. Am. Chem. Soc.*, 2012, **134**, 107–110.
3 B. Liu, J. Liu, H.-B. Li, R. Bhola, E. A. Jackson, L. T. Scott, A. Page, S. Irle, K. Morokuma and C. Zhou, *Nano Lett.*, 2015, **15**, 586–595.
4 H. Omachi, T. Nakayama, E. Takahashi, Y. Segawa and K. Itami, *Nat. Chem.*, 2013, **5**, 572–576.
5 (*a*) J. R. Sanchez-Valencia, T. Dienel, O. Gröning, I. Shorubalko, A. Mueller, M. Jansen, K. Amsharov, P. Ruffieux and R. Fasel, *Nature*, 2014, **512**, 61–64; (*b*) J. Tomada, T. Dienel, F. Hampel, R. Fasel and K. Amsharov, *Nat. Commun.*, 2019, **10**, 3278.
6 X. Yu, J. Zhang, W. Choi, J.-Y. Choi, J. M. Kim, L. Gan and Z. Liu, *Nano Lett.*, 2010, **10**, 3343–3349.
7 L. T. Scott, *Pure Appl. Chem.*, 2017, **89**, 809–820.
8 C.-S. Chen and W.-Y. Yeh, *Chem. – Eur. J.*, 2016, **22**, 16425–16428.
9 (*a*) S.-i Iwamatsu, T. Uozaki, K. Kobayashi, S. Re, S. Nagase and S. Murata, *J. Am. Chem. Soc.*, 2004, **126**, 2668–2669; (*b*) Z. Xiao, G. Ye, Y. Liu, S. Chen, Q. Peng, Q. Zuo and L. Ding, *Angew. Chem., Int. Ed.*, 2012, **51**, 9038–9041.
10 (*a*) Y. Hashikawa, S. Sadai and Y. Murata, *Org. Lett.*, 2021, **23**, 9586–9590; (*b*) Y. Hashikawa, N. Fujikawa and Y. Murata, *J. Am. Chem. Soc.*, 2022, **144**, 23292–23296; (*c*) S. Sadai, Y. Hashikawa and Y. Murata, *Org. Lett.*, 2023, **25**, 2815–2819.
11 (*a*) Y. Yu, L. Xu, X. Huang and L. Gan, *J. Org. Chem.*, 2014, **79**, 2156–2162; (*b*) Z. Liu, Z. Liu, R. Gao, J. Su, Y. Qiu and L. Gan, *Org. Chem. Front.*, 2022, **9**, 320–328.
12 (*a*) Y. Hashikawa, H. Yasui, K. Kurotobi and Y. Murata, *Mater. Chem. Front.*, 2018, **2**, 206–213; (*b*) Y. Hashikawa, S. Okamoto and Y. Murata, *Commun. Chem.*, 2020, **3**, 90; (*c*) Y. Hashikawa and Y. Murata, *Asian J. Org. Chem.*, 2022, **11**, e202200357; (*d*) Y. Hashikawa, N. Fujikawa, S. Okamoto and Y. Murata, *Dalton Trans.*, 2022, **51**, 17804–17808; (*e*) Y. Hashikawa, S. Sadai, S. Okamoto and Y. Murata, *Angew. Chem., Int. Ed.*, 2023, **62**, e202215380.
13 (*a*) A.-C. Bédard, A. Vlassova, A. C. Hernandez-Perez, A. Bes-sette, G. S. Hanan, M. A. Heuft and S. K. Collins, *Chem. – Eur. J.*, 2013, **19**, 16295–16302; (*b*) M. Dračínský, J. Storch, V. Církva, I. Císařová and J. Sýkora, *Phys. Chem. Chem. Phys.*, 2017, **19**, 2900–2907.
14 J. Ohtaka, T. Sakamoto and Y. Kikugawa, *Tetrahedron Lett.*, 2009, **50**, 1681–1683.
15 (*a*) K. Kurotobi and Y. Murata, *Science*, 2011, **333**, 613–616; (*b*) Y. Hashikawa, M. Murata, A. Wakamiya and Y. Murata, *J. Am. Chem. Soc.*, 2017, **139**, 16350–16358.
16 (*a*) Y. Hashikawa and Y. Murata, *Chem. Sci.*, 2020, **11**, 12428–12435; (*b*) Y. Hashikawa, S. Okamoto and Y. Murata, *Chem. – Eur. J.*, 2021, **27**, 4864–4868; (*c*) Y. Hashikawa, H. Kawasaki and Y. Murata, *Organometallics*, 2022, **41**, 354–359.